

RSC Advances



This is an *Accepted Manuscript*, which has been through the Royal Society of Chemistry peer review process and has been accepted for publication.

Accepted Manuscripts are published online shortly after acceptance, before technical editing, formatting and proof reading. Using this free service, authors can make their results available to the community, in citable form, before we publish the edited article. This *Accepted Manuscript* will be replaced by the edited, formatted and paginated article as soon as this is available.

You can find more information about *Accepted Manuscripts* in the [Information for Authors](#).

Please note that technical editing may introduce minor changes to the text and/or graphics, which may alter content. The journal's standard [Terms & Conditions](#) and the [Ethical guidelines](#) still apply. In no event shall the Royal Society of Chemistry be held responsible for any errors or omissions in this *Accepted Manuscript* or any consequences arising from the use of any information it contains.

Cite this: DOI: 10.1039/c0xx00000x

www.rsc.org/xxxxxx

ARTICLE TYPE

Synthesis of imprinted monolithic column with high level of monomers in ionic liquid

Xiu-Yuan Li, Xiu-Xiu Chen, Dan-Dan Zhong, Yan-Ping Huang* and Zhao-Sheng Liu*^b*Received (in XXX, XXX) Xth XXXXXXXXX 20XX, Accepted Xth XXXXXXXXX 20XX*

DOI: 10.1039/b000000x

MIP monolith with good permeability was successfully achieved using a strategy of high content of monomers in [BMIM][BF₄]-based green solvent. The imprinted monolith was prepared with ketoprofen or naproxen as template, 4-vinylpyridine as the functional monomer, and ethylene glycol dimethacrylate as crosslinking monomer. Column efficiency and permeability of the MIP monolith can be tuned by a mixture of [BMIM][BF₄]/ DMSO. The approach allowed the creation of an imprinting system in a short polymerization time (<1.5 h) and higher imprinting factor (8.64) than the MIP prepared in traditional volatile solvent. The textural and morphology of the MIP monoliths of high level of monomers, such as median pore diameter, pore volumes, and pore size distributions, were studied. The influence of polymerization parameters, such as the ratio of template to functional monomer, and the ratio of comonomer to functional monomer on the column performance of the resultant MIP was also investigated.

Introduction

Molecular imprinting technology (MIT) provides a unique opportunity for designing polymers with tailored recognition properties and predetermined selectivity to a target molecule, named the template.¹ The principle of the design of molecularly imprinted polymers (MIPs) allows a degree of customization compared to natural receptors, such as antibodies or enzymes that are capable of recognizing complex biomolecules. As a result, these artificial receptors exhibit the high selectivity for the template, and possess exceptional physical and chemical stability. In addition to the robustness and ease of preparation of MIPs, another major advantage of MIT is that the large diversity of the possible molecular structures can be imprinted. Therefore, MIT have drawn great attention and been widely developed in many fields such as chromatographic stationary phase,² sensor materials,³ enzyme-like catalysis,⁴ drug delivery⁵ since the pioneering work of Wulff in 1970s.

MIPs monolithic column is imprinted stationary phase prepared with a mode of in situ polymerization,⁶ which is based on the technique for fabricating the chromatographic stationary phase of the fourth generation and regarded as a promising approach with high performance. Compared with conventional MIPs, the MIP monoliths possess many merits including simple

preparation, high utilization rate due to avoiding the grinding and sieving, as well as the capability of reducing the density of nonselectivity sites.⁷ In addition, MIP monolith can be manipulated at high flow rate when applying HPLC due to high permeability derived from the its unique pore structure of bimodal pore size distribution. Up to date, MIPs monoliths have attracted a large interest as chiral stationary phase⁸ and selective material for solid phase extraction.⁹ However, the effective imprinted sites of MIP monoliths prepared with these porogenic solvent, i.e., number of cavities per column are rather limited due to greater porosity derived from the monolithic format. Simple method to increase the imprinted sites per column is to decrease the ratio of porogen in pre-polymerization mixture. However, conventional porogenic system can not afford monolithic column with good column permeability prepared with such high content of monomers. In contrast, ultra-high column pressure was observed on the MIP monolith with high content of monomers, not applying to HPLC at all.

Ionic liquid (IL) is a unique, environmentally friendly solvent of low vapor pressure with excellent solvation qualities and chemical/thermal stability.¹⁰ The unusual solvation properties displayed by IL have been attributed to the maintenance of a supramolecular structure in the liquid phase. In addition, IL has been shown to be able to accelerate the polymerization and the magnitude of the rate constant increases with increasing mole fraction of IL in the reaction mixture.¹¹ Recently, neat IL has been used in precipitation polymerization to form MIP nano- or micro-particles,¹² which has proven highly attractive because it provide rapider preparation method, the ability to generate MIPs at low temperature, and better controllability to particle size. It was also found that MIP prepared in ILs showed an increase in favorable template-functional monomer interactions by limiting those associated with non-specific binding. Therefore, the preparation of MIPs in IL is expected to be good porogenic solvent to control morphology and create porosity in a different way from conventional porogens. However, to form a MIP monolith high level of monomer and crosslinker in ionic liquid is still a challenge while traditional MIP monolith can be obtained by combining IL with volatile solvent, e.g., organic small molecules.¹³⁻¹⁵

In present study, we proposed a simple approach for the synthesis of imprinted monolithic column, which is based on interrupting polymerization of an imprinting system containing high weight fractions of the monomers in non-volatile solvent.

This method allowed the amount of monomers in the polymerization mixture set beyond 80%, i.e., only 20% porogenic solvent and the polymerization completed in 1.5 hour. To show proof-of-principle for our strategy, a model of noncovalent molecular imprinting system was chosen because of its versatility in generating MIPs, including adaptable and rapid synthesis, close resemblance to the molecular recognition mechanisms of natural receptors, and the availability of substantial functional monomer libraries. Typically, ketoprofen (KET), 4-vinylpyridine (4-VP), ethylene glycol dimethacrylate (EDMA), and a mixture of 1-butyl-3-methylimidazoliumtetrafluoroborate ([BMIM][BF₄]), one of the most commonly used IL, and non-volatile DMSO (4:1, v/v) was adopted as the template, functional monomer, crosslinker, and porogenic solvent, respectively.

Results and discussion

Among the imidazolium-based IL investigated with varying cation alkyl chain length (C4-C16) containing same anion (BF₄), [BMIM][BF₄] was found a unique solvent to afford good permeability for the resulting monolithic MIP prepared with low ratio of porogenic solvent. To solve adequate amount of the template, DMSO was added in the polymerization system. Too high content (33%) of DMSO in the porogenic solvent led to high column pressure (500 psi under a flow velocity of 0.2 ml/min), while too low content (13%) of DMSO could not dissolve the template thoroughly. It was found that 23% DMSO was the optimal ratio to prepare the MIP monolith.

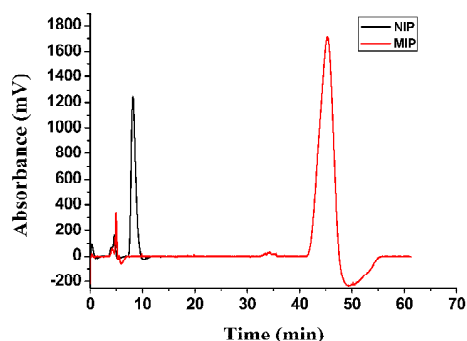


Fig. 1 Chromatograms obtained from KET on the imprinted and non-imprinted monoliths illustrating the imprinting effect. Mobile phase, acetonitrile/acetate buffer (50 mM, pH 3.6; 99/1, v/v); flow rate, 0.3 mL/min; detection wavelength, 255 nm; column temperature, 25 °C.

High performance liquid chromatography was used to evaluate the imprinting effect of the MIP monolith prepared using 80% monomers and 20% porogenic solvent. As shown in Fig. 1, greater capacity factor for KET ($k = 10.4$) with an imprinting factor of 8.64 was observed on the MIP monolith even in a strong mobile phase of ACN/buffer (pH = 3.6) (99/1, v/v). High column efficiency (above 10,000 plates/m) was also achieved on the KET-imprinted monolith. The high column permeability of the MIP monoliths ($1.33 \times 10^{-4} \text{ mm}^2$) was comparable to those prepared with conventional porogens,^{14,16} which allowed the use of high flow rates at relatively low back pressures. It should be noted that further increasing the polymerization time led to the

decrease in imprinting factor and column efficiency of the resulting MIP monolith and increased backpressure.

In present work, the ratio of the weight fractions of the monomers to the solvent in the polymerization mixture was beyond 80%. We called this material made with the ratio as high-density-of-monomer monolith (HDM). Corresponding monolith prepared with conventional porogen content (60%) in identical chemical composition was referred as low-density-of-monomer monolith (LDM). For comparison, a conventional MIP monolith was prepared with 40 wt % monomers and 60 wt % solvent in the porogenic mixture with same ratio of [BMIM][BF₄]/DMSO (77:23) as HDM MIP. In contrast to short polymerization time (<1.5 h) of the HDM MIP monolith, the polymerization for the preparation of the LDM had to be prolonged about 15 h to achieve desired separation ability. The column permeability of the resulting LDM MIP monolith ($1.12 \times 10^{-4} \text{ mm}^2$) was comparable to the HDM MIP monolith ($1.33 \times 10^{-4} \text{ mm}^2$). Furthermore, on the LDM MIP, KET was eluted quickly with an imprinting factor of 4.02, lower than the HDM MIP.

In consistent with the content of monomers in pre-polymerization mixture, bulk density of the HDM MIP was 0.92 g/mL, about twice as much as the LDM MIP (0.49 g/mL). Thus, in spite of higher density of polymer in column, good permeability of the [BMIM][BF₄]-based monolithic MIP was still obtained. Due to identical monomers composition of the HDM and LDM MIP, we presumably attributed the increased imprinting effect to greater density of imprinting sites or a result of a tighter template-monomer cluster as a function of the higher reaction concentration, showing the merit of the HDM monolithic column beyond conventional LDM MIP.

IL [BMIM][BF₄] was found to be the unique porogen to achieve the MIP monolith with desired chromatographic behaviors that traditional porogens can not afford monolithic column in such high content of monomers. This might be attributed to low degree of polymer swelling in ionic liquid,¹² which is markedly different from MIPs prepared with traditional porogen. Using one of the most frequently used porogenic system, a mixture of isooctane/toluene (20/80, v/v),¹⁷ with low content of porogenic solvent (20%) identical to [BMIM][BF₄]-based MIP monolith, the MIP monolith produced indicated very low column permeability and the column pressure of the MIP monolith was 620 psi even with a flow velocity of 0.2 ml/min.

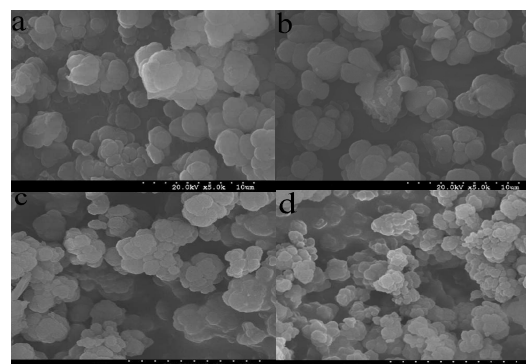


Fig. 2 Morphologies of KET-imprinted polymers (2000 magnifications). (a) HDM-MIP; (b) HDM-NIP; (c) LDM-MIP; (d) LDM-NIP.

The morphology of the KET-imprinted monolith made with high level of monomer and crosslinker, and the corresponding NIP monolith was observed by SEM, respectively. As shown in Fig. 2, the HDM MIP showed extremely large pores located between the agglomerates, confirming the high permeability of the monolith. The size of the microglobules was in the range of 2-4 μm . A comparison of the morphology of the HDM and LDM MIP indicated that the globule size of the MIP monolith can be affected by the ratio of the weight fractions of monomers to the solvent.

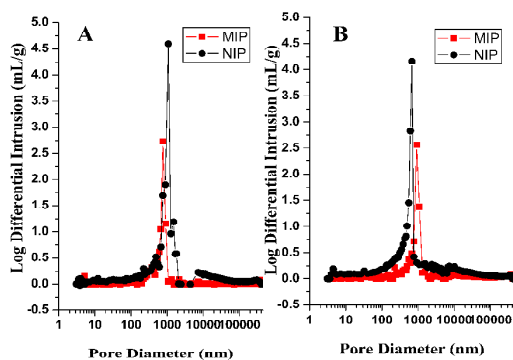


Fig. 3 Differential pore size distribution curves of KET-imprinted monoliths (A) HDM MIP and NIP and (B) LDM MIP and NIP.

To investigate the influence of the varied ratio of porogenic solvent to monomers, pore size distribution of the different monoliths were measured by mercury porosimetry. The differences in pore size distribution curves could be seen between the HDM MIP and NIP prepared without the template (Fig. 3), indicating that the presence of the template affected the formation of macropore due to pre-organization of monomers around the imprinting molecule. The mode pore size of the HDM MIP, i.e., the pore diameter at the maximum of the pore distribution curve, was 1100 nm. In contrast, the mode pore size of the LDM MIP was larger (ca 700 nm). The results suggested that the phase separation in the mixture with a low content of solvents may start early in the polymerization process¹⁸ than with a conventional monomer concentration due to the use of the unique solvent, [BMIM][BF₄], as porogen. Thus, better permeability on the HDM MIP can be demonstrated by the greater pore size, in spite of lower value of pore size than the LDM MIP.

To demonstrate the versatility of the new method for the preparation of MIP monolith, a HDM monolithic column with naproxen (NAP) imprints was prepared according to the recipe same as the KET-imprinted monolith just replacing the template used. The results of chromatographic analysis of the NAP-imprinted monolithic column showed the obvious imprinting effect (IF = 3.52) and greater column permeability than the KET-imprinted monolith. The difference in column permeability may be the result of polymerization kinetic derived from different local concentration of functional monomer induced by preorganization with KET or NAP. In contrast, for the NAP-LDM MIP, lower imprinting factor can be found in spite of similar column permeability.

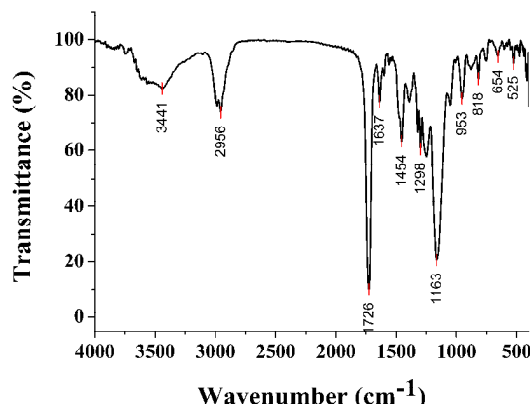


Fig. 4 ATR-FTIR spectra of HDM MIP with KET imprints. A typical FT-IR spectrum of a templated polymer is given in Fig. 4. The presence of significant peaks at approximately 1726 cm^{-1} (C = O stretching), 1298 cm^{-1} , and 1163 cm^{-1} (C–O–C stretching) supported the existence of poly(EDMA) in the MIPs. The characteristic peaks corresponding to C = N stretching (1637 cm^{-1}) and C = C stretching (1454 cm^{-1}) in the pyridine rings could also be observed in the spectra, revealing that poly(4-VP) was also present in the MIPs.

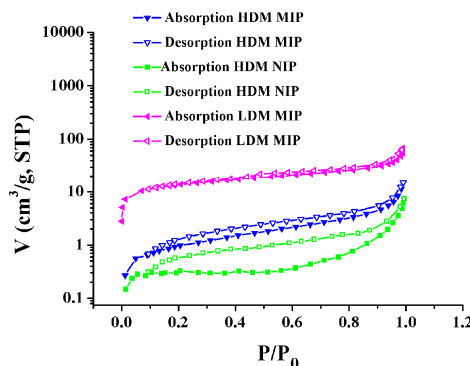


Fig. 5 Nitrogen adsorption-desorption isotherms for HDM MIP, HDM NIP and LDM MIP at 77 K.

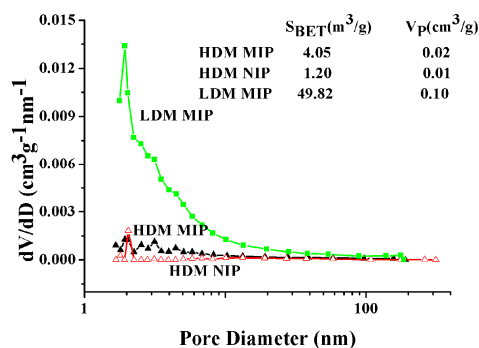


Fig. 6 Pore size distribution curve obtained from the desorption branches of the isotherms for HDM MIP, HDM NIP and LDM MIP at 77 K.

70

To investigate the difference of pore structure between the HDM and LDM MIP further, the pore detail of the NAP-imprinted monolith was studied by N₂ adsorption experiments. Fig. 5 shows N₂ adsorption-desorption isotherms for the samples of the HDM MIP, HDM NIP, and LDM MIP. All three samples gave rise to incomplete type II isotherms with type H3 hysteresis loops, similar to the desorption isotherms of the MIP monolithic materials synthesized using volatile solvent as the porogen.¹⁵ The type of hysteresis loops suggested that the monoliths prepared with the IL [BMIM][BF₄] was porous materials with specific structure of slit-shapes pores.¹⁹ BET surface area of the HDM MIP was 4.05 m²/g, calculated from the adsorption data. In addition, the pore volume of the HDM MIP was 0.02 cm³/g with a pore diameter of about 13 nm (Fig. 6). Corresponding HDM NIP gave a smaller BET surface area (1.2 m²/g), pore volume (0.01 cm³/g) but greater pore diameter (19 nm). In contrast, LDM MIP displayed a greater BET surface area (49.82 m²/g), pore volume (0.10 cm³/g) but smaller pore diameter (9.8 nm). This difference in the morphology of HDM and LDM MIP here might be due to different kinetics of monomers polymerization in the high or low level of ionic liquids in pre-polymerization mixture.²⁰ Apparently, the presence of the template affected the pore structure of the resulting MIP monolith significantly.

Table 1

Capacity factor and imprinting factor of KET on the imprinted and non-imprinted monoliths with the different ratio of MMA-4-VP and EDMA

M:C	k (MIP)	k (NIP)	IF = $k_{\text{MIP}}/k_{\text{NIP}}$
1 : 4	5.177	1.321	3.92
1 : 4.5	9.703	1.533	6.33
1 : 5	6.201	1.309	4.74
1 : 6	2.808	0.856	3.28

Mobile phase, acetonitrile-acetate buffer (50 mmolL⁻¹, pH 3.6) (99:1, v/v); flow rate, 0.3 mLmin⁻¹; detection wavelength, 255 nm; temperature, 25 °C

It should be noted that using 4-VP as functional monomer solely in the polymerization system studied here caused a bristle monolith. Thus, to overcome the problem, non-functional monomer, methyl methacrylate, MMA, was used as co-monomer in the pre-polymerization mixture by replacing the part of 4-VP. The effect of ratio of co-monomer to functional monomer on the affinity of HDM MIP was investigated by chromatographic analysis. As shown in the Table 1, the imprinting factors of the HDM MIPs made with different ratio of co-monomer to functional monomer ranged from 3.28 to 6.33. The maximum imprinting factor was obtained when the ratio of co-monomer to functional monomer (MMA/4-VP) was 4:5. This result was in agreement with ref.²¹, which was attributed to that the non-functional monomers can occupy the positions in the binding sites where polar groups are not needed for the interactions with the ligand.

The effect of template-to-monomer (T/M) molar ratio on the imprinting factor of the resulting MIP monoliths has been found to be important with regard to the number and quality of

Table 2

Capacity factor and imprinting factor of KET and its structural analogues with the different ratio of template and monomer

Monoliths	T:M	k_{KET}	k_{FENO}	k_{NAP}	k_{FENBI}	k_{IBU}	IF
C1	1:7.2	5.676	4.645	3.882	2.392	2.954	3.70
C2	1:6.5	6.393	5.026	4.253	3.327	2.689	4.17
C3	1:6	6.570	5.645	5.976	2.533	3.481	4.29
C4	1:5	9.703	7.583	6.653	5.278	4.079	6.33
C5	-	1.533	1.520	1.519	1.478	1.065	-

Mobile phase, acetonitrile-acetate buffer (50 mmolL⁻¹, pH 3.6) (99:1, v/v); flow rate, 0.3 mLmin⁻¹; detection wavelength, 255 nm; temperature, 25 °C

sites in MIPs.²² In this work, we changed T/M ratio by varying the amount of template in a fixed ratio of 4-VP to EDMA (1:4). As shown in Table 2, the imprinting factor increased with the increase in the amount of the template. However, further increasing the amount of template, e.g., a T/M ratio of 1:2, caused the monolithic column with high back pressure, which can not be evaluated by HPLC. This was in agreement with previous report on the effect of increasing the concentration of template.¹⁶ The best imprinting factor was obtained on the MIP prepared with a molar ratio of 1:5. In contrast to the major effect of the template used in imprinting on column permeability of MIP monolith,²³ for the system studied here, the data of monolith permeability clearly indicated that the amount of template had less effect on the morphology of the resulting monolith.

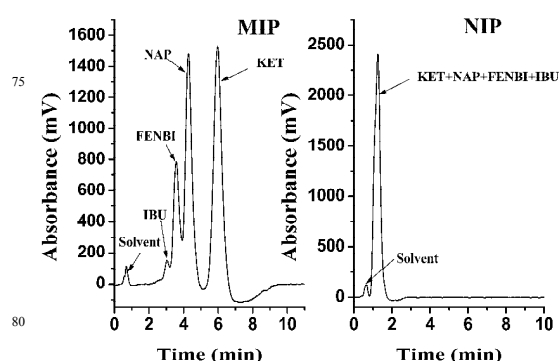


Fig. 7 Separation of KET and its structural analogues on the KET-imprinted HDM MIP and NIP. Mobile phase, acetonitrile/acetate buffer (50 mM, pH 3.6; 99/1, v/v); flow rate, 2.0 mL/ min; detection wavelength, 254 nm; column temperature, 25°C; NAP: naproxen, IBU: ibuprofen, FENBI: fenbifen.

To assess the selectivity of the MIP monolith, affinity screening of structurally similar compounds was investigated on the KET-imprinted HDM MIP. A group of drugs structurally similar to the template was used to simulate a combinatorial library. As shown in Fig. 7, rapid separation of KET from the structurally similar drugs was completed in less than 8 min at a flow of 2 mL min⁻¹. In contrast, the structural analogs were eluted as a single peak on the corresponding NIP, which demonstrated the good selectivity of the KET-imprinted HDM monolith.

The contents of NAP in naproxen capsules were directly determined using the NAP-imprinted monolith. The typical chromatogram of naproxen capsules was shown in Fig. 8. Clearly, the impurity in the capsules and NAP were well-separated and the excellent selectivity was achieved in this NAP-MIP monolithic stationary phase. The determined content of NAP in the naproxen capsules were 49.66%, which is greatly consistent with that claimed and meets the criterion of the state-promulgated pharmacopoeia (2000, Part II, China) very well. These results revealed that the NAP-imprinted monolith can be directly used for selective analysis and determination of NAP in real samples.

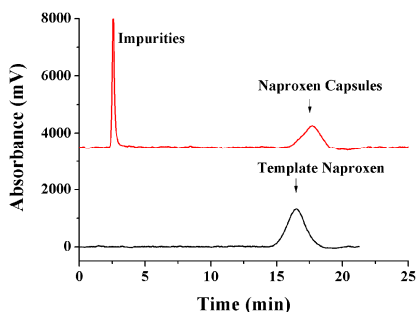


Fig. 8. Separation of imprints and NAP in naproxen capsules using NAP-imprinted monolith (C3). Mobile phase, acetonitrile acetate buffer (50 mmolL⁻¹, pH 3.6) (7:3, v/v); flow rate, 0.2 mLmin⁻¹; detection wavelength, 254 nm; temperature, 28°C.

Conclusions

In summary, we have demonstrated for the first time a facile and highly efficient approach to the synthesis of imprinted monolithic column with high level of monomer and crosslinker. The resulting MIP monolith with good permeability was successfully prepared in a porogenic system containing low content of porogenic solvent to 20%. Furthermore, the approach suggested here allowed the creation of an efficient and highly selective imprinting system in a short polymerization time (<1.5 h) and a greener mode (non-volatile and low content of porogenic solvent), which imprinting effect was comparable to conventional monolithic MIP. Further work should be considered performing the polymerization in new IL to obtain MIP monolith with higher column efficiency for chiral separation.

Experimental

Materials and instruments

Ketoprofen (KET) (98%) was obtained from Zhengjiang Xianju Chemical Reagent (Zhejiang, China). Naproxen (NAP), ibuprofen (IBU), fenbifen (FENBI) and fenoprofen (FENO), were from Wuhan Yuancheng Chemical Reagent (Wuhan, China) (analytical grade). 4-Vinylpyridine (4-VP) (98%) was purchased from Sigma (St. Louis, MO, USA). Ethylene glycol dimethacrylate (EDMA) (98%) was from Tokyo Chemical Industry Co. Ltd. (Tokyo, Japan). 2,2-Azobis (2-isobutyronitrile) (AIBN) (analytical grade) was supplied by Special Chemical Reagent Factory of Nankai University (Tianjin, China). 1-Butyl-3-methylimidazolium tetrafluoroborate ([BMIM][BF₄]) (98%) was purchased from Shanghai Chengjie Chemical Reagent (Shanghai, China). Methyl methacrylate (MMA) (analytical grade) was from Tianjin Kewei Chemical Reagent (Tianjin, China). HPLC-grade acetonitrile (ACN) was from Tianjin Biaoshiqi Chemical Reagent (Tianjin, China). Kermel Chemical Reagent (Tianjin, China) supplied dimethyl sulfoxide (DMSO) (analytical grade). Other analytical reagents were from Tianjin Chemical Reagent Ltd. Co. (Tianjin, China).

Preparation of imprinted monoliths

The MIP monolith was directly prepared by in situ polymerization within the confines of a stainless-steel chromatographic column tube (100 mm × 4.6 mm i.d.). A pre-polymerization mixture was prepared by mixing the template, AIBN, 4-VP, MMA, EDMA, DMSO, and [BMIM][BF₄]. The pre-polymerization mixture was sonicated for 15 min and introduced to the stainless steel column. The ends of the column were sealed and submerged in a 60 °C water bath for different monolithic columns. After polymerization, the column was flushed with acetonitrile to remove any unreacted reagents. The template molecules were removed by washing with a mixture of methanol and acetic acid (9:1, v/v) until no template molecules were detected in the extraction solvent. The blank polymer was synthesized in a similar way in the absence of the template.

Chromatographic evaluation

High performance liquid chromatography was performed with an Angilent 1100 series chromatographic system. Data processing was carried out by a HPCORE workstation and the samples were monitored at 255 nm. All of mobile phases were filtered through a 0.22 μm membrane from Millipore before use. The injection volume was 20 μL and each sample was analyzed three times.

The retention factor, *k*, was calculated by:

$$k = (t_R - t_0)/t_0 \quad (1)$$

where *t_R* is the retention time of retained peak, *t₀* is the retention time of unretained acetone.

The number of theoretical plates (*N*) was calculated by the equation:

$$N = 16 (t_R/W)^2 \quad (2)$$

W is the width at the baseline between tangents drawn to inflection points for the peak.

Imprinting factor (IF) was calculated as $IF = k_{MIP} / k_{NIP}$, where k_{MIP} is the capacity factor of the template molecule eluted from the imprinted polymer and k_{NIP} is the capacity factor of the template molecule eluted from the non-imprinted polymer.

Scanning electron microscopy

Scanning electron microscopy (SEM) was used for characterization of the monoliths. Samples were sputter-coated with gold before obtaining images. All scanning electron micrographic images were obtained by use of a Shimadzu SS-550 scanning electron microscope, operated at 15 kV with a filament current of 60 mA.

Mercury porosimetry

Mercury intrusion and extrusion experiments on the monolithic polymer samples were performed over a wide range for pressures starting in vacuum up to 60,000 psi (1 psi = 6.895×10^{-3} MPa) by a Poremaster 60 instrument (Quantachrome Instruments, Boyton Beach, FL, USA). Data acquisition was performed in autospeed continuous canning mode enabling maximum speed in the absence of intrusion or extrusion and maximum resolution and sufficient equilibration time (sampling time).

Acknowledgments

This work was supported by the National Natural Science Foundation of China (Grant No. 21375096) and supported by the Hundreds Talents Program of the Chinese Academy of Sciences.

Notes and references

Tianjin Key Laboratory on Technologies Enabling Development of Clinical Therapeutics and Diagnostics (Theranostics), School of Pharmacy, Tianjin Medical University, Tianjin 300070, China. Fax: +86+22 2353 6746; Tel: +86+22 2353 6746; E-mail: zhaoshengliu@sohu.com; E-mail: huangyp100@163.com

- J. E. Lofgreen, G. A., Ozin, *Chem. Soc. Rev.*, 2014, **43**, 911; K. Haupt, A.V. Linares, M. Bompert, B.T. Bui, *Top. Curr. Chem.*, 2012, **325**, 1; L. Chen, S. Xu, J. Li, *Chem. Soc. Rev.*, 2011, **40**, 2922; G. Wulff, *Chem. Rev.*, 2002, **102**, 1; G. Wulff, *Angew. Chem. Int. Ed.*, 1995, **34**, 1812.
- B. Tóth, G. Horvai, *Top. Curr. Chem.*, 2012, **325**, 267.
- Y. Fuchs, O. Soppera, K. Haupt, *Anal. Chim. Acta*, 2012, **717**, 7.
- S. Muratsugu, M. Tada, *Acc. Chem. Res.*, 2013, **46**, 300.
- F. Puoci, G. Cirillo, M. Curcio, O.I. Parisi, F. Iemma, N. Picci, *Expert Opin. Drug Deliv.*, 2011, **8**, 1379.
- J. Matsui, T. Kato, T. Takeuchi, M. Suzuki, K. Yokoyama, E. Tamiya, I. Karube, *Anal. Chem.*, 1993, **65**, 2223; B. Sellergren, *Anal. Chem.*, 1994, **66**, 1678.
- H. Kim, G. Guiochon, *Anal. Chem.*, 2005, **77**, 93.
- C. Zheng, Y. P. Huang, Z. S. Liu, *Anal. Bioanal. Chem.*, 2013, **405**, 2147.
- J. Tan, Z.-T. Jiang, R. Li, X.-P. Yan, *TrAC*, 2012, **39**, 207.
- D. D. Patel, J. M. Lee, *Chem. Rec.*, 2012, **12**, 329; Walsh D. A., Lovelock K. R., Licence P., *Chem. Soc. Rev.*, 2010, **39**, 4185; T. Torimoto, T. Tsuda, K. Okazaki, S. Kuwabata, *Adv. Mater.*, 2010, **22**, 1196; M. Armand, F. Endres, D. R. MacFarlane, H. Ohno, B.

- Scrosati, *Nat. Mater.*, 2009, **8**, 621; de M. P. Domínguez, *Angew. Chem. Int. Ed. Engl.*, 2008, **47**, 6960; S. Park, R. J. Kazlauskas, *Curr. Opin. Biotechnol.*, 2003, **14**, 432.
- T. L. Greaves, C. J. Drummond, *Chem. Soc. Rev.*, 2013, **42**, 1096; Z. Hu, C. J. Margulis, *Acc. Chem. Res.*, 2007, **40**, 1097.
- K. Booker, M. C. Bowyer, C. I. Holdsworth, A. McCluskey, *Chem. Commun.*, 2006, **11**, 1730.
- X. Sun, J. He, G. Cai, A. Lin, W. Zheng, X. Liu, L. Chen, X. He, Y. Zhang, *J. Sep. Sci.*, 2010, **33**, 3786; J. Ou, L. Kong, C. Pan, X. Su, X. Lei, H. Zou, *J. Chromatogr. A*, 2006, **1117**, 163; L.Q. Lin, Y.C. Li, Q. Fu, *Polymer*, 2006, **47**, 3792; M. L. Zhang, J. P. Xie, Q. Zhou, G. Q. Chen, Z. Liu, *J. Chromatogr. A*, 2003, **984**, 173.
- L. Ban, L. Zhao, B. L. Deng, Y. P. Huang, Z. S. Liu, *Anal. Bioanal. Chem.*, 2013, **405**, 2245.
- L. H. Bai, X. X. Chen, Y. P. Huang, Q. W. Zhang, Z. S. Liu, *Anal. Bioanal. Chem.*, 2013, **405**, 8935; D. D. Zhong, Y. P. Huang, X. L. Xin, Z. S. Liu, H. A. Aisa, *J. Chromatogr. B*, 2013, **934**, 109.
- L. Zhao, L. Ban, Q. W. Zhang, Y. P. Huang, Z.S. Liu, *J. Chromatogr. A*, 2011, **1218**, 9071.
- A. Seebach, A. Seidel, *Anal. Chim. Acta*, 2007, **591**, 57; Y.-P. Huang, S.-J. Zhang, L. Zhao, Q.-W. Zhang, Z.-S. Liu, *Chromatographia*, 2010, **71**, 559.
- G. Guiochon, *J. Chromatogr. A*, 2007, **1168**, 101; F. Gritti, G. Guiochon, *J. Chromatogr. A*, 2012, **1228**, 2.
- K.S.W. Sing, *Pure Appl. Chem.*, 1982, **54**, 2201.
- K. Booker, M. C. Bowyer, C. J. Lennard, C. I. Holdsworth, A. McCluskey, *Aust. J. Chem.*, 2007, **60**, 51.
- P. Spégel, L. Schweitz, S. Nilsson, *Electrophoresis*, 2001, **22**, 3833; L. Schweitz, L. I. Andersson, S. Nilsson, *Analyst* 2002, **127**, 22; X.-X. Shi, L. Xu, H.-Q. Duan, Y.-P. Huang, Z.-S. Liu, *Electrophoresis*, 2011, **32**, 1348.
- B. Sellergren, *J. Chromatogr. A*, 2001, **906**, 227; H.S. Andersson, J.G. Karlsson, S. A. Piletsky, A.-C. Koch-Schmidt, K. Mosbach, I. A. Nicholls, *J. Chromatogr. A*, 1999, **848**, 39.
- J. Haginaka, A. Futagami, *J. Chromatogr. A*, 2008, **1185**, 258.